Ligand- and solvent-free ATRP of MMA with $FeBr_3$ and inorganic salts

Jirong Wang,[†] Xiaolin Xie,[†] Zhigang Xue,*[,†] Christophe Fliedel,[‡] and Rinaldo Poli*[,‡]

[†]Key Laboratory for Material Chemistry of Energy Conversion and Storage, Ministry of Education, School of Chemistry and Chemical Engineering, Huazhong University of Science and Technology, Wuhan 430074, P. R. China

[‡]CNRS, LCC (Laboratoire de Chimie de Coordination), Universitéde Toulouse, UPS, INPT, 205 Route de Narbonne, BP 44099, F-31077 Toulouse Cedex 4, France

SUPPORTING INFORMATION

Materials. Methyl methacrylate (MMA, 98+%, Sinpharm) and *n*-butyl methacrylate (BMA, 98+%, Sinpharm) were passed through a column filled with neutral alumina, dried over calcium hydride (CaH_2), distilled under reduced pressure and stored in a freezer under argon. Ethyl α-bromophenylacetate (EBrPA, 95%, Alfa Aesar), ethyl α-bromoisobutyrate (EBriB, 98%, Alfa Aesar), methyl 2-bromoisobutyrate (MBriB, 95+%, Alfa Aesar), (1-bromoethyl)benzene (PEBr, 97%, Alfa Aesar), ethyl 2-bromopropionate (EBrP, 98%, Alfa Aesar), methyl 2-bromopropionate (MBrP, 98%, Alfa Aesar), 2-bromopropionitrile (BPN, 98%, Alfa Aesar), 2-chloropropionitrile (CPN, 98%, Alfa Aesar), iron(III) bromide ($FeBr_3$, 98+%, Alfa Aesar), iron(III) chloride ($FeCl_3$, 98+%, Alfa Aesar), iron(III) chloride hexahydrate ($FeCl_3$ $6H_2O$, 99.95%, Macklin) and 2,2,6,6-tetramethylpiperidine 1-oxy (TEMPO, 98%, Sigma Aldrich) were used as received without further purification. The inorganic bases and salts sodium carbonate (Na_2CO_3), sodium bicarbonate ($NaHCO_3$), potassium carbonate (K_2CO_3), potassium bicarbonate ($KHCO_3$), potassium hydroxide (KOH), sodium hydroxide (NaOH), potassium phosphate (K_3PO_4), lithium chloride (LiCl), sodium chloride (NaCl), potassium chloride (KCl), lithium bromide (LiBr), sodium bromide (NaBr), potassium bromide (KBr), rubidium bromide (RuBr) and cesium bromide (CsBr) (all from Sinpharm) were also used as received.

Instrumentation. ^1H and ^{13}C NMR spectroscopy was performed using Bruker AV400, AdvanceIII400 HD and Varian INOVA-400 MHz spectrometers with deuterated chloroform as the solvent. The spectra were calibrated using the solvent resonances and the resonance values are reported on the δ scale (ppm) with positive values upfield from the tetramethylsilane (TMS) standard. The $M_{n,GPC}$ and M_w/M_n of the

polymers were determined by GPC using either an Agilent 1100 gel permeation chromatograph, with a PLgel 79911GP-104 column (7.5 mm × 300 mm, 10 μm bead size) or a Shimadzu system equipped with a Shimadzu RID-20A refractive index detector with two PSS SDV analytical columns (1000 Å and 100000 Å, 5 μm, 8 × 300 mm). THF was used as the eluent at a flow rate of 1 mL/min at 35°C. The GC-MS analyses were conducted on a QP2010 Ultra GC/MS apparatus from Shimadzu equipped with a 30 m capillary column (Phenomenex, Zebron, ZB-5ms, fused silica capillary column, 30 M × 0.25 mm × 0.25 mm film thickness) with acetonitrile as the solvent.

General polymerisation procedure. Unless otherwise stated, a typical system consisted of $[monomer]_0/[FeBr_3]_0/[initiator]_0/[inorganic\ additive]_0$ = 200:0.25:1:2. A Schlenk flask (25 mL) was charged under argon with the salt and sealed by a rubber septum. Then the degassed monomer and initiator were added through degassed syringes. The solution was stirred for 20 min at room temperature. After three freeze-pump-thaw cycles, the flask was immersed in a thermostatic oil bath at 60°C. The salt is generally incompletely dissolved in the reaction medium. At timed intervals, samples were withdrawn from the flask with a degassed syringe. The monomer conversion was determined gravimetrically after the removal of the unconverted monomer under reduced pressure. The resulting residue was diluted with tetrahydrofuran (THF) and then filtered through a column filled with neutral aluminium oxide to remove any insoluble salt. The poly(methyl methacrylate) (PMMA) product was then precipitated by adding excess *n*-hexane and collected by filtration, then dried under vacuum overnight at 80°C for the gel permeation chromatographic (GPC) characterisation.

Table S1. Raw data for the bulk $FeBr_3$-catalyzed and EBrPA-initiated MMA polymerization in the presence of alkali metal carbonates (Figure 1 and Figure S2).[a]

Time (min)	MMA conversion	Ln([M]$_0$/[M])	$M_{n,th}$	$M_{n,GPC}$	Đ
1. Na_2CO_3	y = 0.0016x - 0.1961; R^2 = 0.9839				
240	19.8	0.2206	3965	3900	1.11
330	28.3	0.3327	5667	5300	1.12
390	33.7	0.4110	6748	6400	1.12
510	45.2	0.6015	9050	8200	1.11
630	54.1	0.7787	10833	9900	1.12
690	62.1	0.9702	12434	11300	1.1
2. K_2CO_3	y = 0.0012x - 0.0665; R^2 = 0.9900				
180	14.3	0.1543	2863	2600	1.11
270	23.3	0.2653	4665	3900	1.12
360	30.3	0.3610	6067	5500	1.12
450	38.5	0.4861	7709	6500	1.11
540	42.3	0.5499	8470	7600	1.12
630	51.3	0.7195	10272	8700	1.1
3. Na_2CO_3 (in the dark)	y = 0.0023x - 0.1378; R^2 = 0.9990				
120	14.4	0.1555	2883	2158	1.06
210	28.4	0.3341	5687	3423	1.09
300	43	0.5621	8610	5330	1.09
390	53.5	0.7657	10712	6267	1.1
450	59.6	0.9063	11934	8577	1.09
510	65.3	1.0584	13075	9840	1.06

[a] [MMA]:[$FeBr_3$]:[Cat_2CO_3]:[EBrPA] = 200:0.25:2:1 (Cat = Na, K), T = 60°C.

Table S2. Raw data for the chain extension of a PMMA-Br macroinitiator in bulk MMA.[a]

Time (min)	MMA conversion	$Ln([M]_0/[M])$	$M_{n,th}$	$M_{n,GPC}$	Đ
	y = 0.0010x - 0.0591; R^2 = 0.9975				
0	0	0	-		
120	11.3	0.1199	13656	14400	1.11
240	14.6	0.1578	15308	15000	1.11
480	18.6	0.2058	17311	16500	1.12
720	23.4	0.2666	19714	19000	1.10

[a] [MMA]:[$FeBr_3$]:[Na_2CO_3]:[PMMA-Br] = 500:0.25:2:1, T = 60°C.

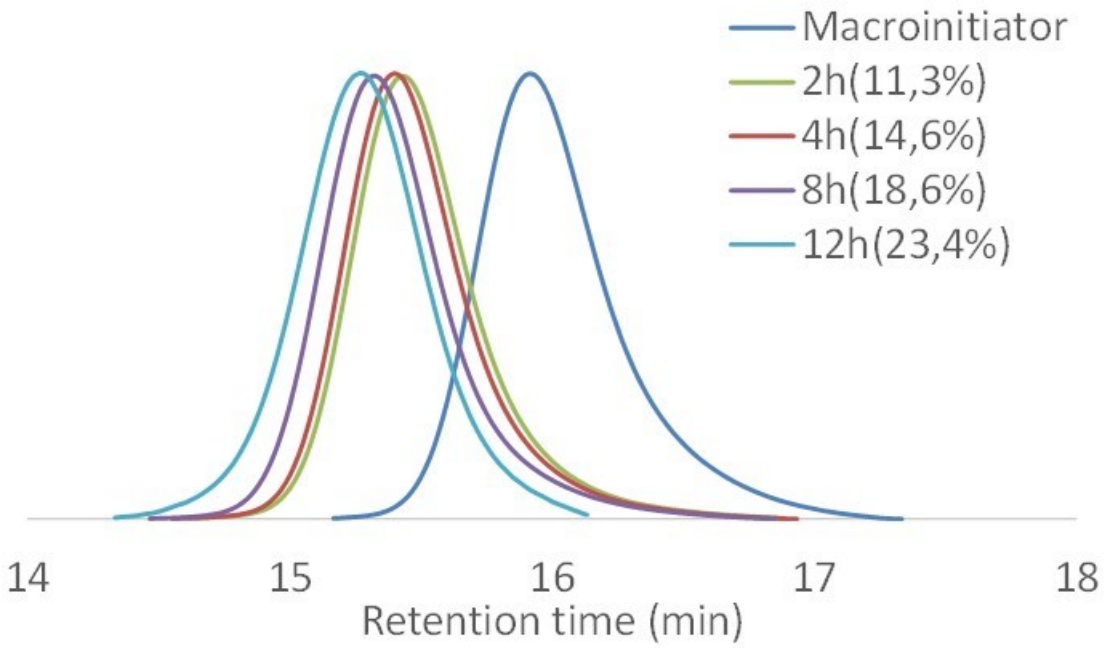

Figure S1. GPC traces for the chain extension of a PMAA-Br in bulk MMA with $FeBr_3/Na_2CO_3$ (data in Table S2).

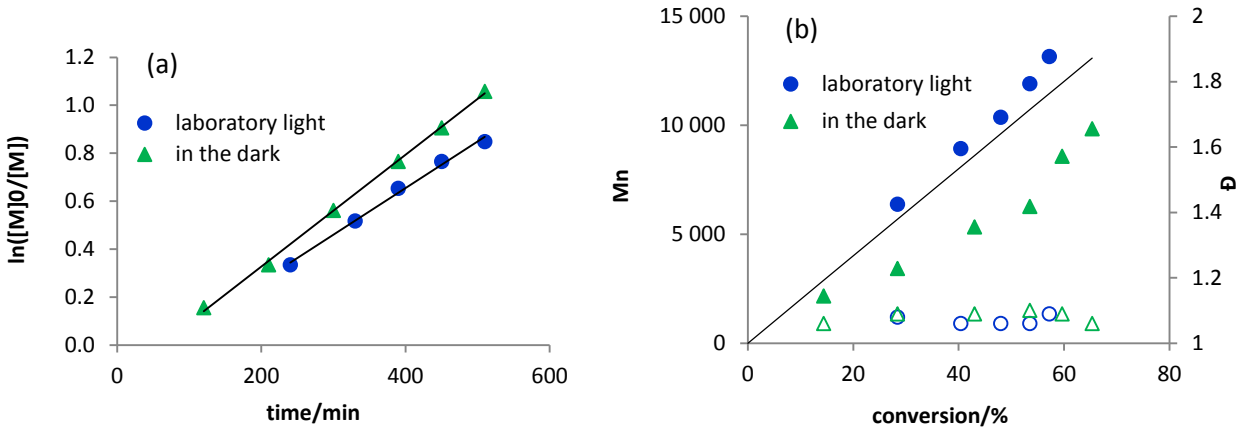

Figure S2. First-order plots (a) and evolution of M_n and $Đ$ with conversion (b) for the MMA polymerizations carried out in the presence of $FeBr_3/Na_2CO_3$ with and without laboratory light (data in Table S1).

Table S3. Raw data for the EBrPA-initiated bulk MMA polymerization in the presence of $FeBr_3/Na_2CO_3$ at different MMA/EBrPA ratios.[a]

Time (min)	MMA conversion	Ln([M]$_0$/[M])	$M_{n,th}$	$M_{n,GPC}$	Đ
x = 200	See Table S1				
x = 400	y = 0.0010x - 0.0591; R^2 = 0.9975				
270	18.6	0.2058	7449	6200	1.13
360	25.6	0.2957	10252	8200	1.13
450	32.9	0.3990	13175	10300	1.12
540	39	0.4943	15618	12400	1.11
630	43.3	0.5674	17340	14000	1.1
720	48	0.6539	19222	14900	1.1
x = 600	y = 0.0012x - 0.1872; R^2 = 0.9877				
240	11.9	0.1267	7148	7900	1.17
330	18	0.1985	10813	11700	1.15
420	24.4	0.2797	14657	16600	1.13
540	37.5	0.4700	22526	23500	1.13
630	44.9	0.5960	26971	27400	1.13
720	48.8	0.6694	29314	30100	1.12
x = 800	y = 0.0011x - 0.2555; R^2 = 0.9876				
330	11.6	0.1233	9291	10200	1.17
450	22.1	0.2497	17700	18600	1.23
540	29.3	0.3467	23467	26200	1.29
660	36.5	0.4541	29234	31700	1.46
750	45.8	0.6125	36682	38100	1.27
x = 1000	y = 0.0005x - 0.1314; R^2 = 0.9958				
420	10	0.1054	10012	8600	1.13
600	15.3	0.1661	15318	13900	1.09
1380	45.1	0.5997	45152	37600	1.08

[a] [MMA]:[$FeBr_3$]:[Na_2CO_3]:[EBrPA] = x:0.25:2:1, T = 60°C.

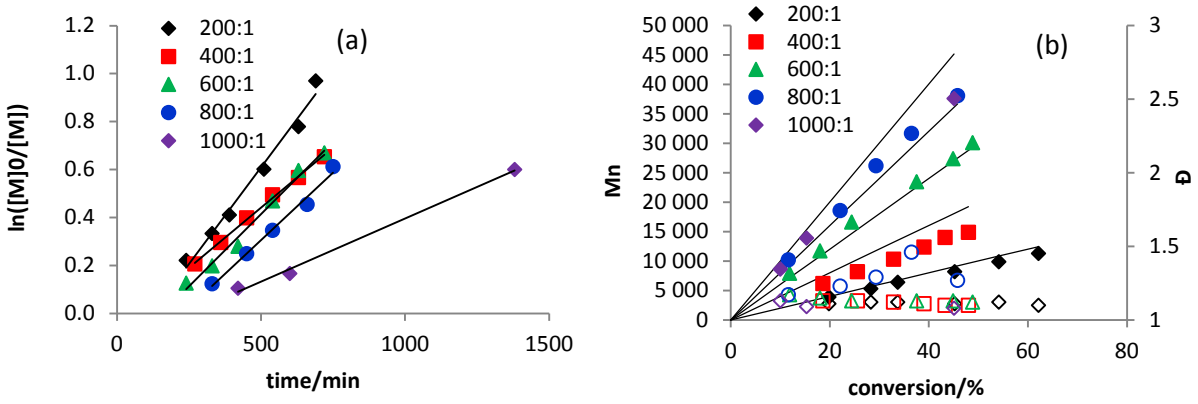

Figure S3. First-order plots (a) and evolution of M_n and $Đ$ with conversion (b) for the experiments in Table S3.

Table S4. Raw data for the bulk $FeBr_3$-catalyzed MMA polymerization in the presence of Na_2CO_3 and various initiators.[a]

Time (min)	MMA conversion	Ln([M]$_0$/[M])	$M_{n,th}$	$M_{n,GPC}$	Đ
1. EBrPA	See Table S1				
2. EBiB	y = 0.0007x - 0.1148; R^2 = 0.9780				
360	14.6	0.1578	2923	5700	1.16
450	19.9	0.2219	3985	7000	1.16
540	25.7	0.2971	5146	8200	1.15
690	31	0.3711	6207	9100	1.13
780	38.8	0.4910	7769	10100	1.18
3. MBiB	y = 0.0018x - 0.4638; R^2 = 0.8630				
360	22.8	0.2588	4565	6800	1.17
450	30.2	0.3595	6047	8200	1.15
540	38.4	0.4845	7689	10700	1.14
690	46.3	0.6218	9271	12200	1.14
780	67.5	1.1239	13516	15000	1.12
4. BPN	y = 0.0011x - 0.1677; R^2 = 0.9343				
360	21.2	0.2383	4245	5400	1.15
450	27.2	0.3175	5446	6500	1.17
540	34.8	0.4277	6968	7900	1.14
690	39.6	0.5042	7929	9000	1.15
780	52.2	0.7381	10452	10500	1.13
5. EBrP	y = 0.0050x - 0.5542; R^2 = 0.9464				
120	10.7	0.1132	2142	12000	1.27
180	24.8	0.2850	4966	22600	1.22
210	34.4	0.4216	6888	29600	1.19
240	47.5	0.6444	9511	30600	1.27
270	58	0.8675	11613	35300	1.26
6. MBrP	y = 0.0010x - 0.1662; R^2 = 0.9980				
270	8.9	0.0932	1782	8600	1.26
330	13.7	0.1473	2743	11000	1.29
510	28.9	0.3411	5787	17000	1.31
750	42.5	0.5534	8510	21900	1.19
6. PEBr	y = 0.0092x - 0.7579; R^2 = 0.9679				
120	32.7	0.3960	6548	12400	1.26
150	43	0.5621	8610	14000	1.25
165	51.6	0.7257	10332	18700	1.24
180	59.2	0.8965	11854	20100	1.22
195	66.1	1.0818	13235	21900	1.19

[a] [MMA]:[$FeBr_3$]:[Na_2CO_3]:[Initiator] = 200:0.25:2:1, T = 60°C.

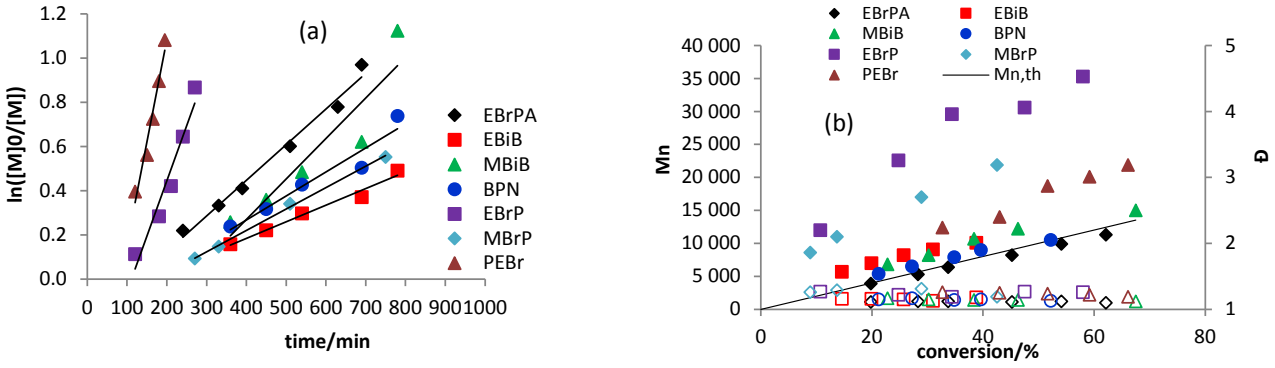

Figure S4. First-order plots (a) and evolution of M_n and $Đ$ with conversion (b) for the experiments in Table S4.

Table S5. Raw data for the bulk EBrPA-initiated MMA polymerization in the presence of $FeBr_3/Na_2CO_3$ at different temperatures (Figure 2).[a]

Time (min)	MMA conversion	$Ln([M]_0/[M])$	$M_{n,th}$	$M_{n,GPC}$	Đ
1. 60°C	See Table S1				
2. 70°C	$y = 0.0031x - 0.2263$; $R^2 = 0.9905$				
120	17	0.1863	3404	4000	1.17
180	28.9	0.3411	5787	6400	1.14
210	34.2	0.4186	6848	7400	1.13
270	44.1	0.5816	8830	9300	1.12
330	52.1	0.7361	10432	11000	1.12
390	61.4	0.9519	12294	13100	1.08
450	68	1.1394	13616	14600	1.11
510	75.8	1.4188	15178	15800	1.13
3. 80°C	$y = 0.0045x - 0.0235$; $R^2 = 0.9763$				
60	18.5	0.2046	3704	4200	1.18
90	33.6	0.4095	6728	7100	1.13
120	41.7	0.5396	8350	8700	1.13
150	45.9	0.6143	9191	9600	1.14
180	57.4	0.8533	11493	12000	1.12
240	63.9	1.0189	12795	13200	1.12
4. 90°C	$y = 0.0045x - 0.0235$; $R^2 = 0.9763$				
45	20.8	0.2332	4165	4700	1.13
75	33.1	0.4020	6628	6900	1.12
105	42.7	0.5569	8550	8700	1.13
135	51.3	0.7195	10272	10300	1.14
165	58.7	0.8843	11754	11800	1.14
195	62.9	0.9916	12595	13500	1.17
270	73	1.3093	14617	15500	1.17

[a] $[MMA]:[FeBr_3]:[Na_2CO_3]:[EBrPA] = 200:0.25:2:1$.

Table S6. Raw data for the bulk EBrPA-initiated MMA polymerization in the presence of $FeBr_3/Na_2CO_3$ with different $Na_2CO_3/FeBr_3$ ratios (Figure 3).[a]

Time (min)	MMA conversion	$Ln([M]_0/[M])$	$M_{n,th}$	$M_{n,GPC}$	Đ
1. x = 0.5	y = 0.0005x + 0.0590; R^2 = 0.9839				
180	12.1	0.1290	2423	2500	1.12
240	17.3	0.1900	3464	3600	1.13
330	18.9	0.2095	3784	3900	1.14
420	21.5	0.2421	4305	4400	1.14
750	33.3	0.4050	6668	6700	1.12
2. x = 2	See Table S1				
3. x = 3	y = 0.0016x - 0.1391; R^2 = 0.9872				
180	13.4	0.1439	2683	2800	1.12
240	22.5	0.2549	4505	4600	1.12
300	28.9	0.3411	5787	5800	1.14
360	33.8	0.4125	6768	7100	1.13
480	44.1	0.5816	8830	9300	1.11
600	58.5	0.8795	11714	11900	1.12
720	62.2	0.9729	12454	12600	1.12

[a] [MMA]:[$FeBr_3$]:[Na_2CO_3]:[EBrPA] = 200:0.25:x:1; T = 60°C.

Table S7. Raw data for the bulk EBrPA-initiated MMA polymerization in the presence of $FeBr_3/Na_2CO_3$ with different $FeBr_3$/EBrPA ratios (Figure 4).[a]

Time (min)	MMA conversion	$Ln([M]_0/[M])$	$M_{n,th}$	$M_{n,GPC}$	Đ
1. x = 0.25	See Table S1				
2. x = 0.5	y = 0.0013x - 0.0668; R^2 = 0.9763				
180	15.3	0.1661	3064	2900	1.14
300	27.1	0.3161	5426	5100	1.10
420	38.8	0.4910	7769	7900	1.14
480	47.3	0.6406	9471	9600	1.12
660	54.3	0.7831	10873	11000	1.12
3. x = 0.75	y = 0.0015x - 0.2181; R^2 = 0.9845				
270	17.5	0.1924	3504	2800	1.14
360	27.4	0.3202	5486	3900	1.15
480	38.3	0.4829	7669	5800	1.12
630	48.5	0.6636	9711	7800	1.12
720	59	0.8916	11814	8700	1.12
4. x = 1	y = 0.0005x - 0.0231; R^2 = 0.9939				
240	9.7	0.1020	1942	1800	1.14
300	12.7	0.1358	2543	2300	1.13
390	17.5	0.1924	3504	3100	1.13
510	21.1	0.2370	4225	4000	1.12
660	28.1	0.3299	5627	5400	1.13

[a] [MMA]:[$FeBr_3$]:[Na_2CO_3]:[EBrPA] = 200:x:2:1; T = 60°C.

Table S8. Raw data for the bulk EBrPA-initiated MMA polymerization in the presence of $FeBr_3$ and different inorganic salts and bases.

Time (min)	MMA conversion	Ln([M]$_0$/[M])	$M_{n,th}$	$M_{n,GPC}$	Đ
1. $NaHCO_3$ [a]	y = 0.0009x - 0.0379; R^2 = 0.9632				
210	8.1	0.0845	1622	2557	1.08
330	18.9	0.2095	3785	4252	1.12
450	29.3	0.3467	5867	5726	1.12
570	43.5	0.5709	8710	7571	1.08
1320	64.9	1.0470	12995	11899	1.1
2. $KHCO_3$ [a]	y = 0.0008x - 0.0303; R^2 = 0.9826				
210	9	0.0943	1802	2403	1.09
330	17.9	0.1972	3584	3751	1.10
450	28.9	0.3411	5787	4878	1.11
570	38.2	0.4813	7649	5800	1.11
1320	62.1	0.9702	12434	11742	1.06
3. K_3PO_4 [a]	y = 0.0018x - 0.4709; R^2 = 0.9960				
330	8.7	0.0910	1742	2183	1.04
450	29.3	0.3467	5867	6679	1.16
570	48	0.6539	9611	10657	1.16
1320	85.7	1.9449	17160	18866	1.26
4. NaOH [a]					
120	7.0		1645	3344024	2.07
5. KOH [a]					
120	9.3		2105	749173	1.49
6. NaOH [b]	y = 0.0009x + 0.0486; R^2 = 0.9816				
120	10.3	0.1087	2062	1900	1.17
240	24.5	0.2810	4906	4200	1.12
300	27.8	0.3257	5566	5200	1.13
390	34.3	0.4201	6868	5900	1.12
480	35.4	0.4370	7088	6400	1.14
600	41.9	0.5430	8390	7300	1.12
720	47.5	0.6444	9511	8700	1.13
840	54.2	0.7809	10853	9700	1.12
7. KOH [b]	y = 0.0009x + 0.0486; R^2 = 0.9816				
120	12.7	0.1358	2543	2265	1.08
240	24.4	0.2797	4886	3683	1.13
360	35.1	0.4323	7028	4849	1.11
480	45.7	0.6106	9151	5157	1.16
600	56.3	0.8278	11273	6084	1.11

[a] [MMA]:[$FeBr_3$]:[salt]:[EBrPA] = 200:0.25:2:1; T = 60°C. [b] [MMA]:[$FeBr_3$]:[salt]:[EBrPA] = 200:1:2:1; T = 60°C.

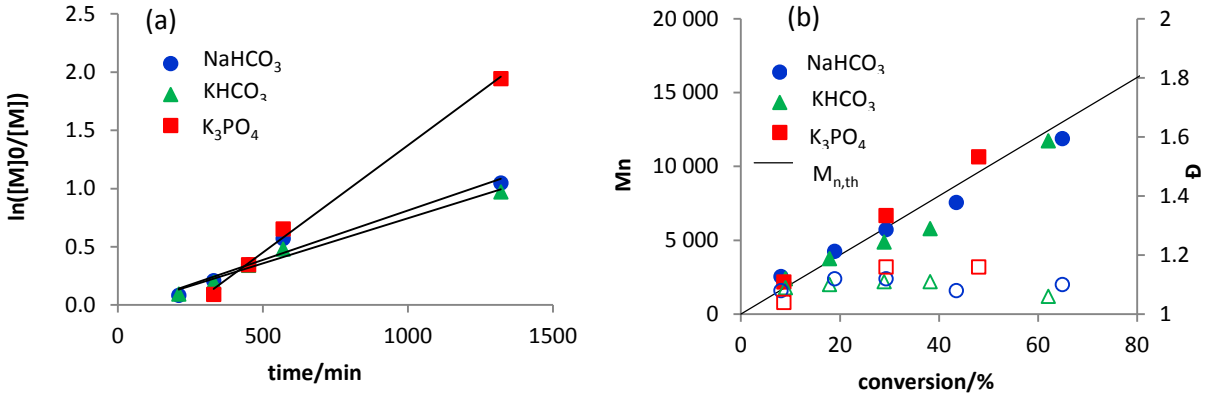

Figure S5. First-order plots (a) and evolution of M_n and $Đ$ with conversion (b) for the EBrPA-initiated polymerizations with $FeBr_3$/salt (bicarbonates, phosphate); data in Table S8.

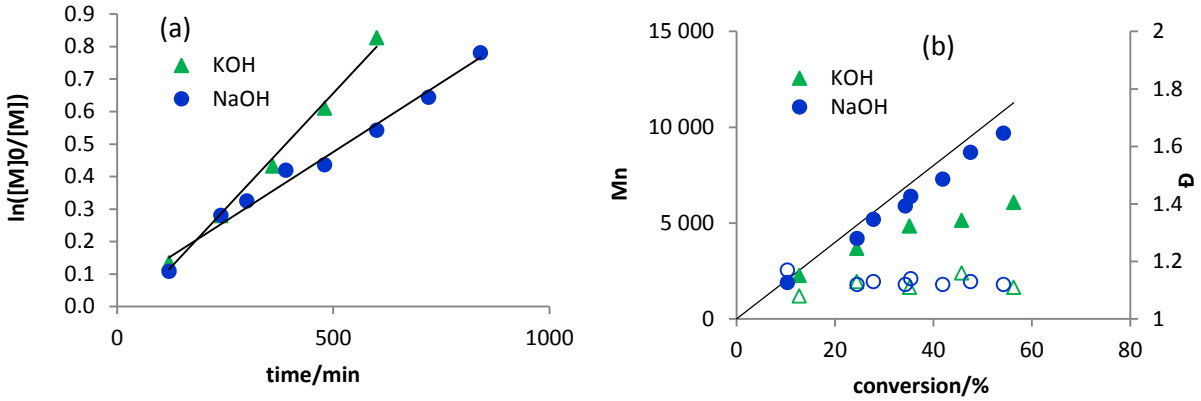

Figure S6. First-order plots (a) and evolution of M_n and $Đ$ with conversion (b) for the EBrPA-initiated polymerizations with $FeBr_3/Cat^+OH^-$ (Cat = Na, K); data in Table S8.

Table S9. Raw data for the bulk EBrPA-initiated MMA polymerization in the presence of $FeBr_3$ of Na and K chlorides and bromides (Figure 5).[a]

Time (min)	MMA conversion	$Ln([M]_0/[M])$	$M_{n,th}$	$M_{n,GPC}$	Đ
1. NaBr	y = 0.0027x + 0.2324; R^2 = 0.9654				
60	31.3	0.3754	6267	5700	1.14
90	37.3	0.4668	7469	7500	1.15
150	46.6	0.6274	9331	9700	1.2
180	54.6	0.7897	10933	11900	1.25
270	60.3	0.9238	12074	12800	1.3
2. KBr	y = 0.0026x + 0.186; R^2 = 0.9977				
60	28.6	0.3369	5727	6100	1.15
90	34.3	0.4201	6868	7300	1.13
150	44.2	0.5834	8850	9300	1.15
210	52.8	0.7508	10572	11000	1.19
270	58.5	0.8795	11714	12300	1.21
3. NaCl	y = 0.0019x + 0.2199; R^2 = 0.9557				
60	26.1	0.3025	5226	5500	1.18
90	31.8	0.3827	6367	7000	1.21
150	42.4	0.5516	8490	8800	1.26
210	48.6	0.6655	9731	10600	1.24
300	53.1	0.7572	10632	11100	1.29
4. NaBr	y = 0.0007x + 0.1981; R^2 = 0.9409				
90	20.3	0.2269	4065	3900	1.2
150	28.7	0.3383	5747	5700	1.21
300	35.3	0.4354	7068	8400	1.26
480	41.1	0.5293	8230	9300	1.34

[a] [MMA]:[$FeBr_3$]:[salt]:[EBrPA] = 200:0.5:4:1; T = 90°C.

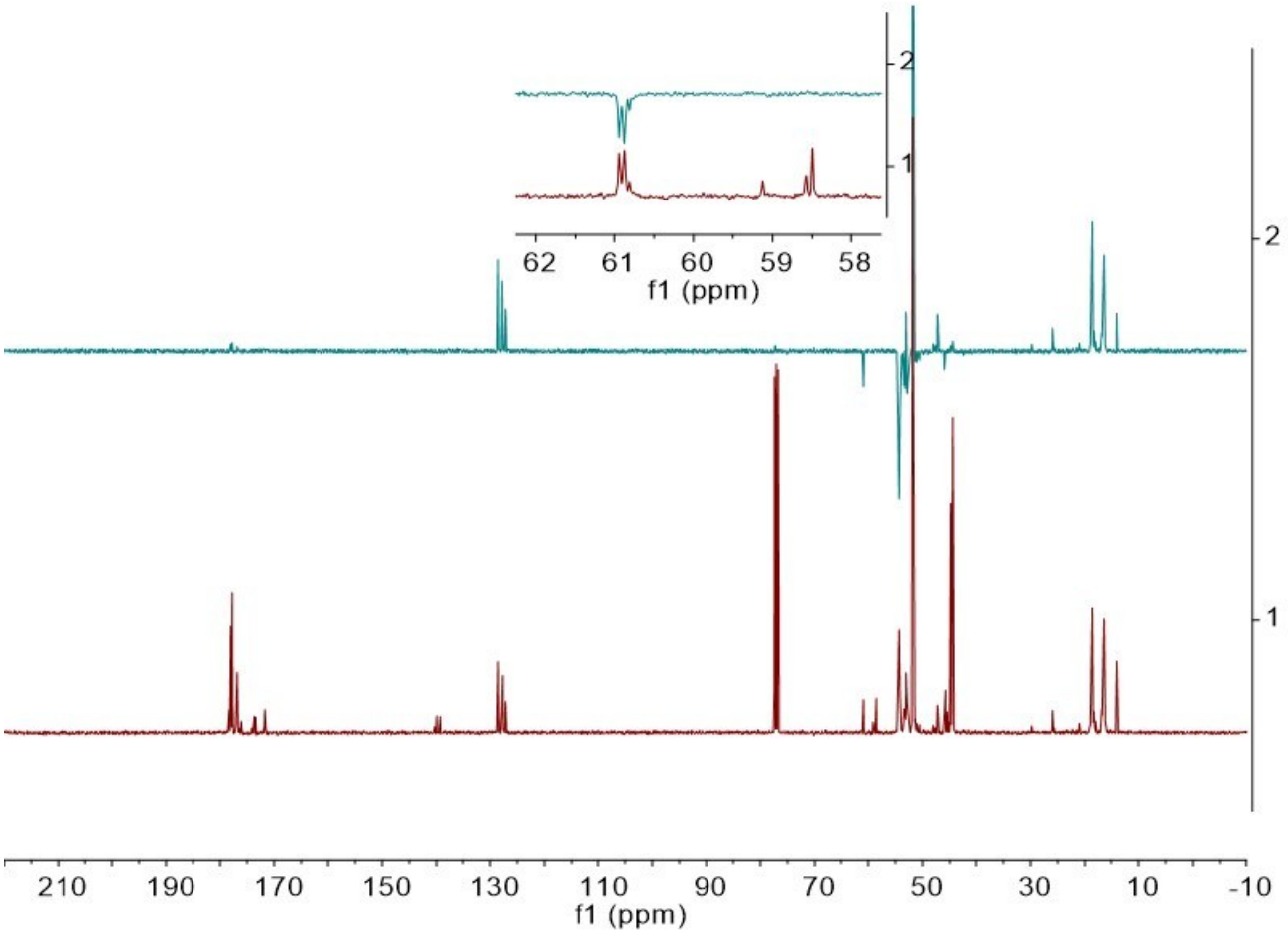

Figure S7. Comparison of the $^{31}C\{^{1}H\}$ and ^{13}C-DEPT135 NMR spectra in $CDCl_3$ of the PMMA-Br (M_n = 2171 g mol^{-1}, $Đ$ = 1.10) produced by bulk polymerization ([MMA]:[$FeBr_3$]:[Na_2CO_3]:[EBrPA] = 50:0.25:2:1) and stopped at 30% conversion.

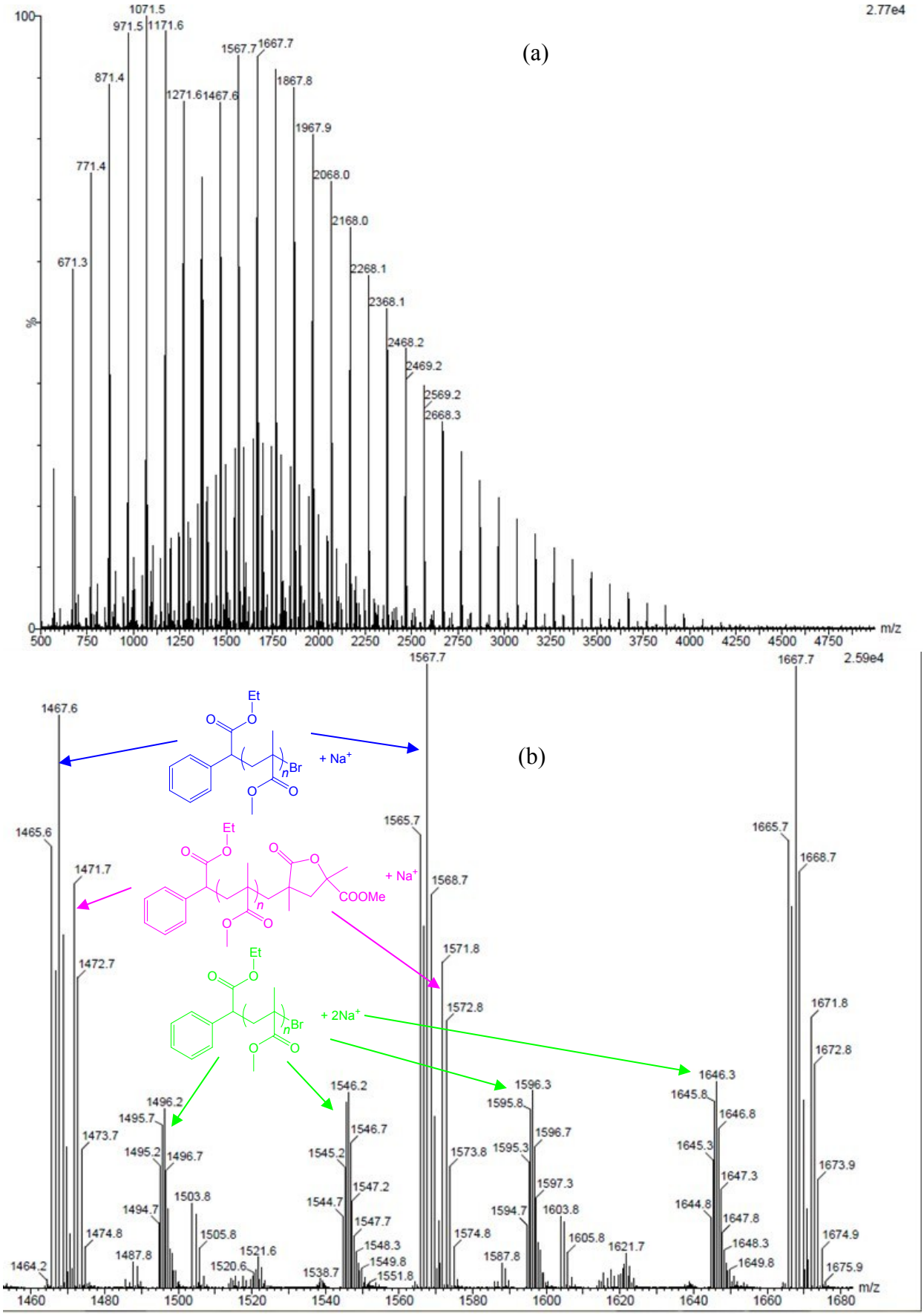

Figure S8. ESI-MS of EPA-MMA_n-Br in $CHCl_3$. (a) Full spectrum in the 1000-5000 m/z range. (b) Excerpt in the 2030-2300 m/z range.

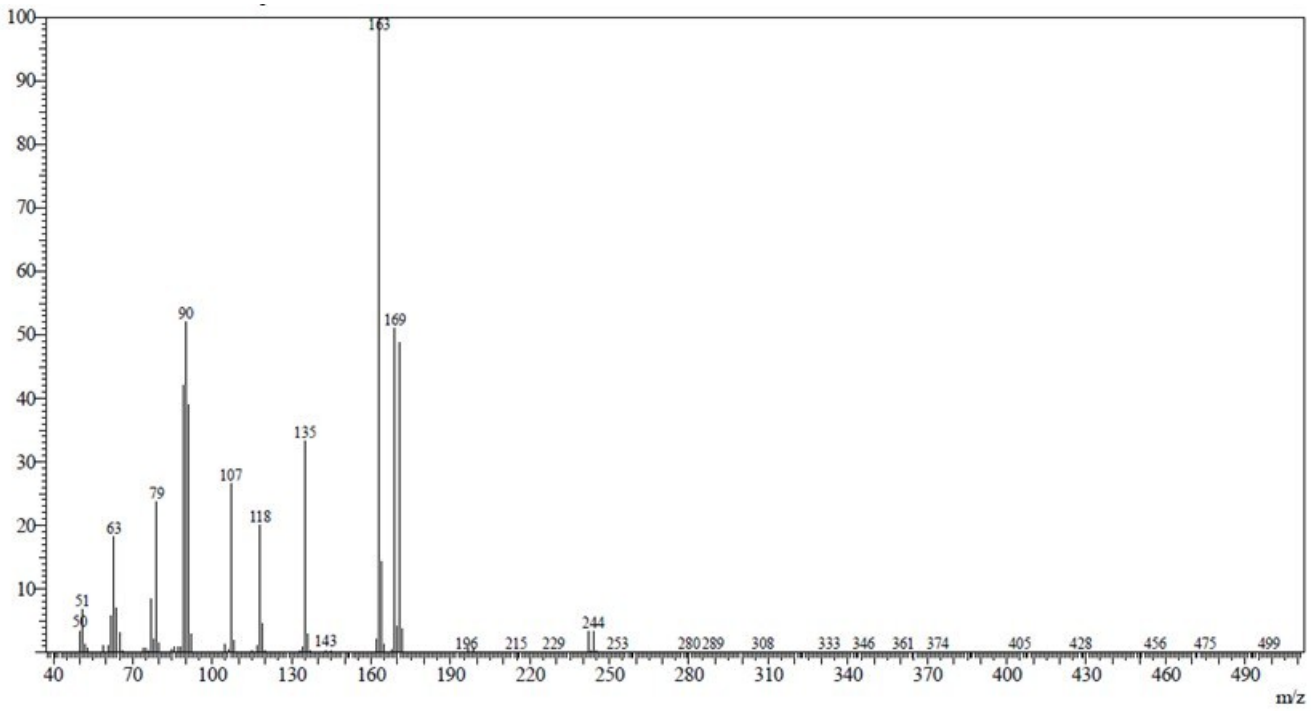

Figure S9. MS of EBrPA (GC peak at 20.70 min in Figure 6.1).

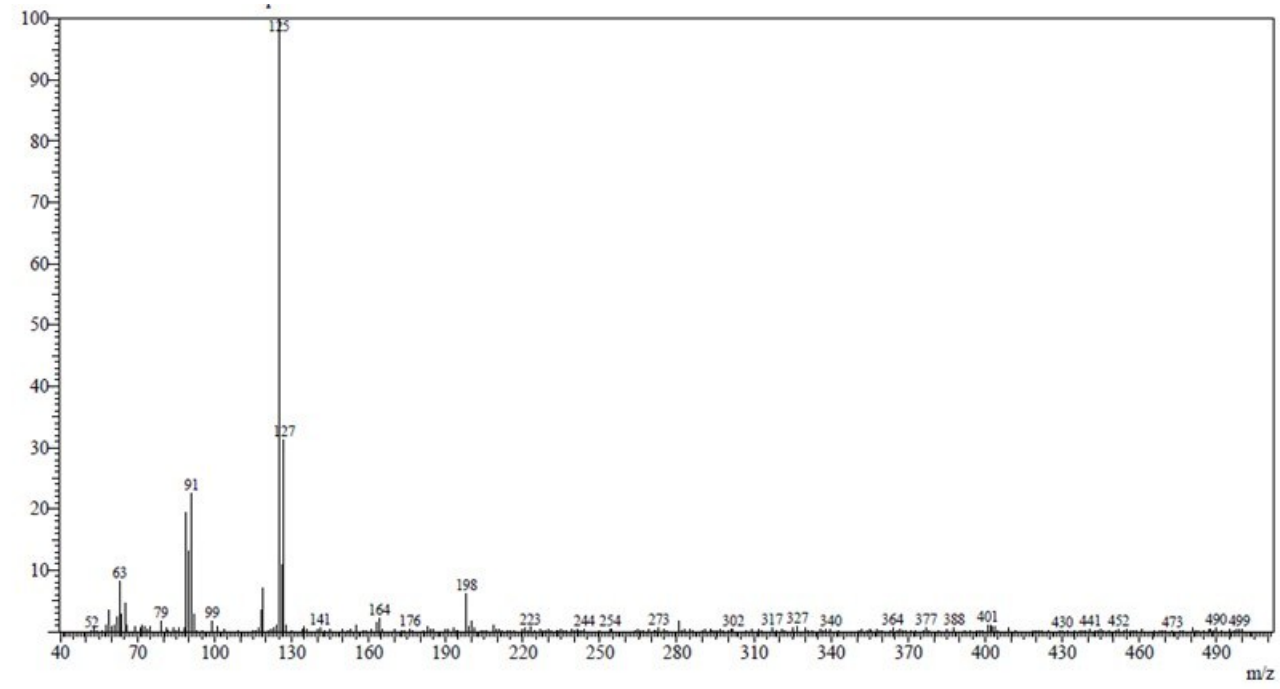

Figure S10. MS of EClPA (GC peak at 19.48 min in Figure 6.2).

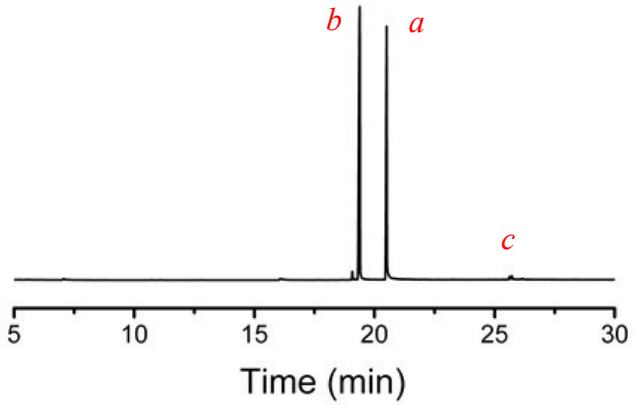

Figure S11. Gas-chromatogram of the solution obtained after heating EBrPA (0.0472 M in MeCN) at 90°C for 2 h in the presence of $FeCl_3 \cdot 6H_2O$ (0.042 M) and KOH (0.086 M).

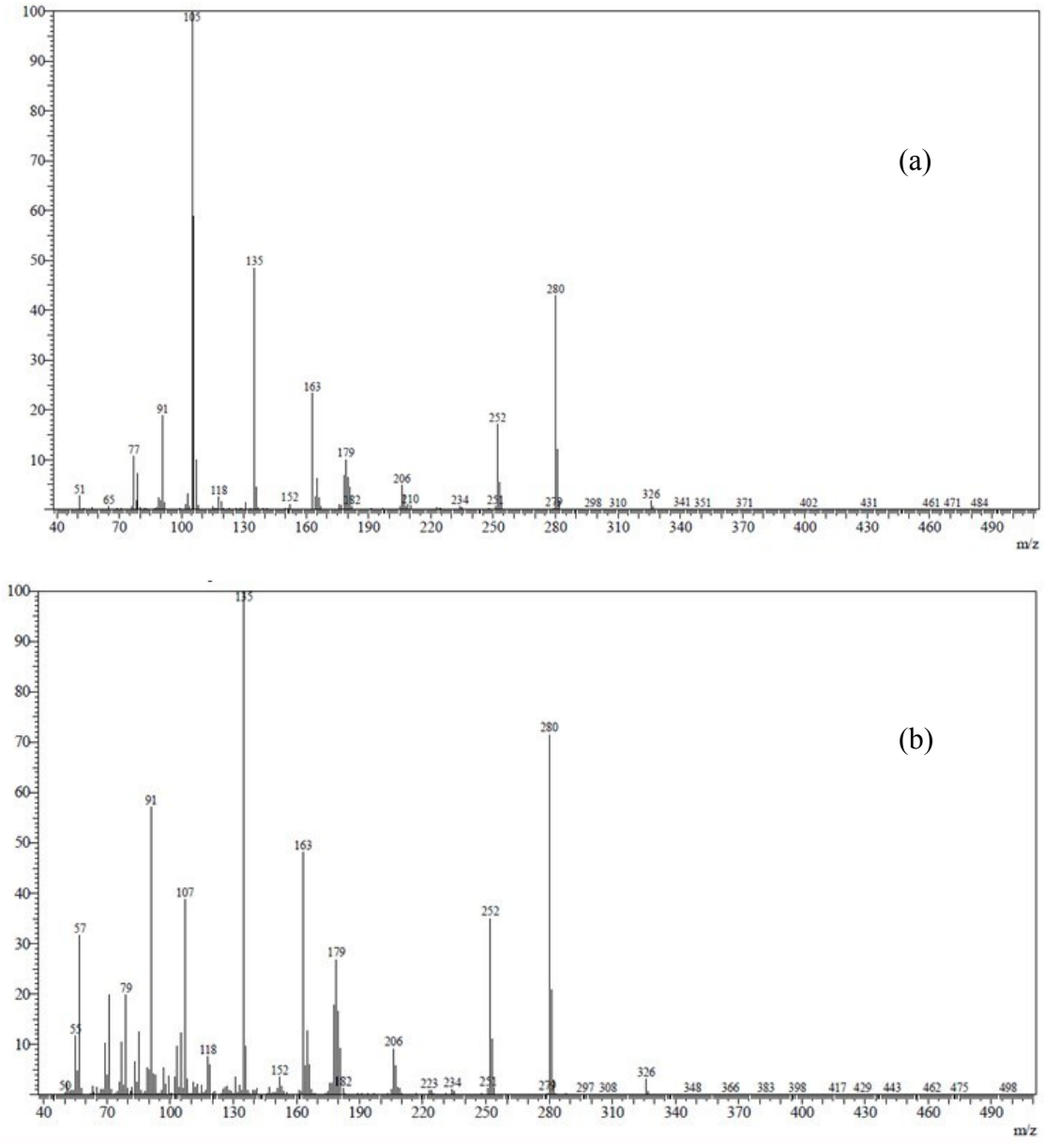

Figure S12. MS of the two peaks *d* (at 25.66 min, *a*, and 25.78, *b* min, respectively) in the GC of Figure 6.3).

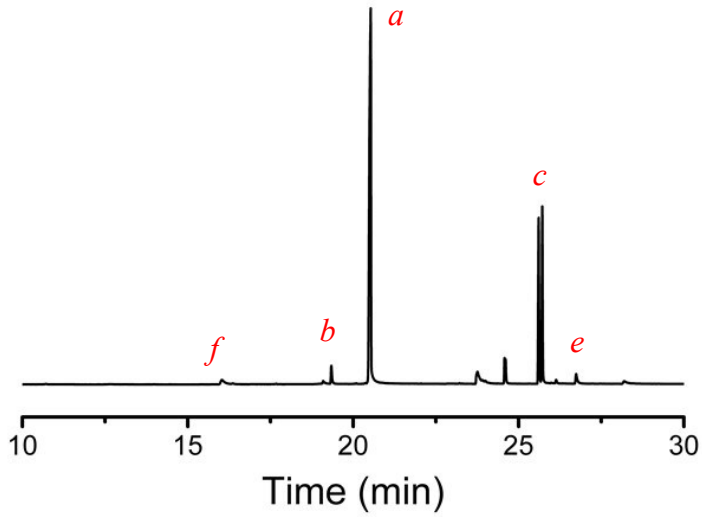

Figure S13. Gas-chromatogram of the solution obtained after heating EBrPA (0.0472 M in MeCN) at 90°C for 2 h in the presence of $FeBr_3$ (0.042 M) and KOH (0.086 M).

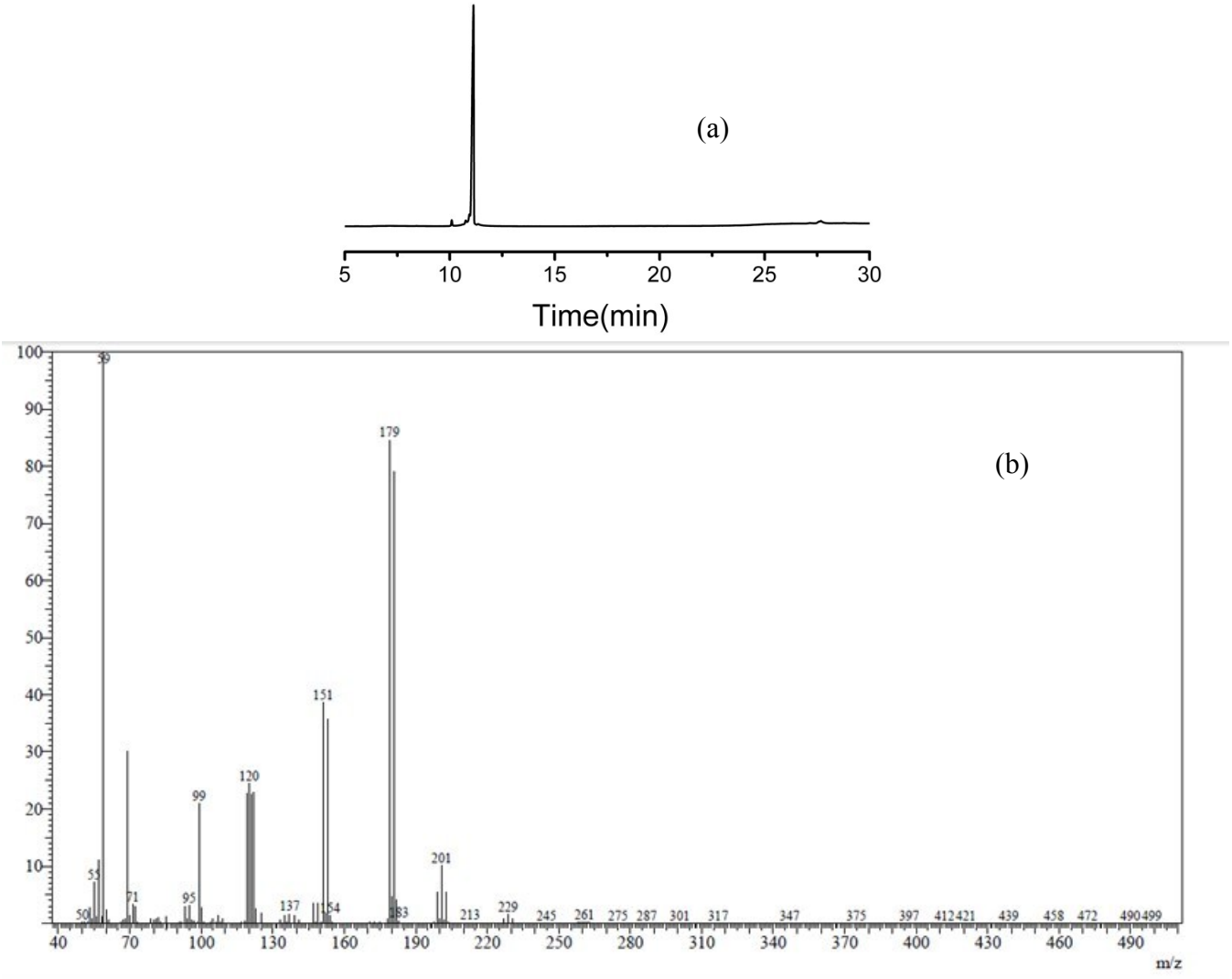

Figure S14. (a) Gas-chromatogram of methyl dibromoisobutyrate (0.042 M in MeCN). (b) MS of the peak eluted at 11.26 min.

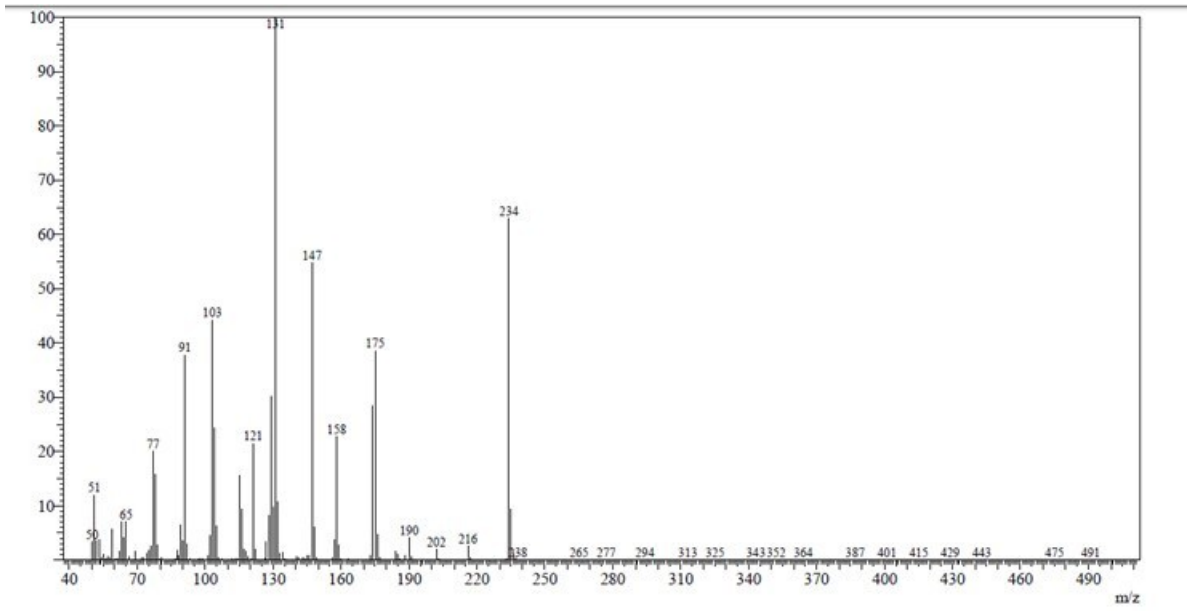

Figure S15. MS of compound *f* (peak at 23.74 min) in the GC of Figure 6.4.

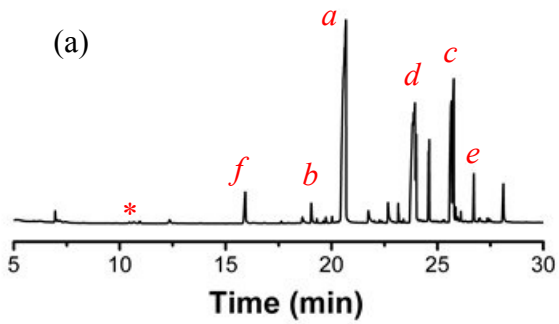

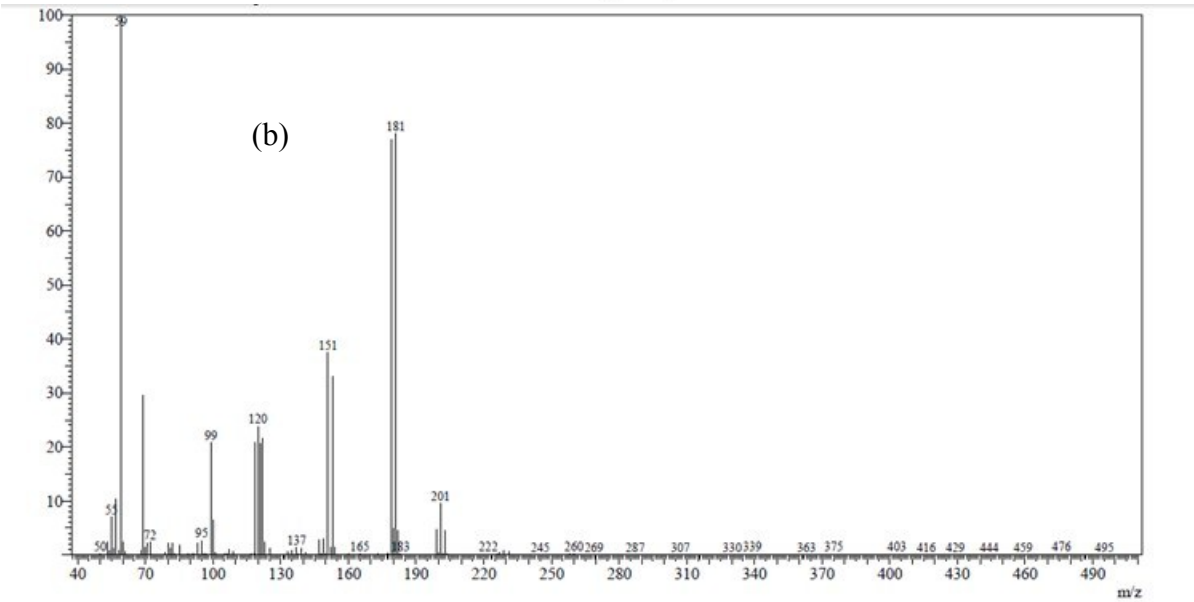

Figure S16. (a) Gas-chromatogram of the solution obtained after heating EBrPA (0.0472 M in MeCN) at 90°C for 2 h in the presence of $FeBr_3$ (0.042 M), KOH (0.086 M) and MMA (0.042 M). The starred peak at 11.26 is due to methyl 1,2-dibromobutyrate. (b) MS of the peak eluted at 11.26 min (*cf.* with the MS of genuine methyl 1,2-dibromobutyrate in Figure S14(b)).

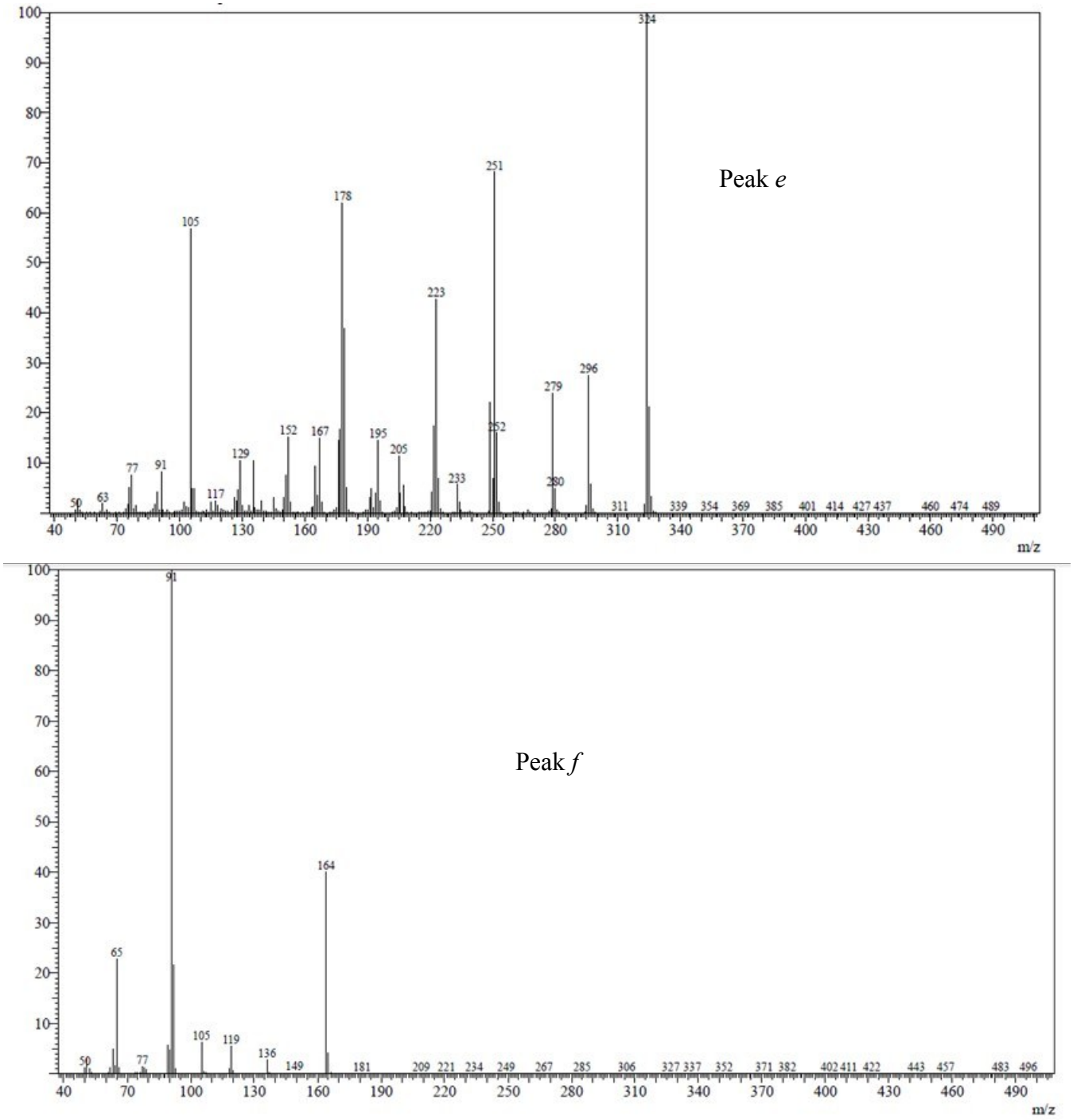

Figure S17. MS of compounds *e* and *f* (peaks at 26.11 and 16.00 min, respectively) in the GC of Figure 7.2).